International Journal of Nanomedicine

Dovepress
open access to scientific and medical research

Open Access Full Text Article

ORIGINAL RESEARCH

Poly (lactic-co-glycolic acid)/graphene oxide composites combined with electrical stimulation in wound healing: preparation and characterization

This article was published in the following Dove Press journal:
International Journal of Nanomedicine

Di You[1]
Kai Li[1]
Wenlai Guo[2]
Guoqing Zhao[1]
Chuan Fu[1]

[1]Department of Anesthesiology, China-Japan Union Hospital of Jilin University, Changchun 130033, People's Republic of China; [2]Department of Hand and Foot Surgery, The Second Hospital of Jilin University, Changchun 130012, People's Republic of China

Purpose: In this study, we fabricated multifunctional, electrically conductive composites by incorporating graphene oxide (GO) into a poly (lactic-co-glycolic acid) (PLGA) copolymer for wound repair. Furthermore, the resultant composites were coupled with electrical stimulation to further improve the therapeutic effect of wound repair.

Methods: We evaluated the surface morphology of the composites, as well as their physical properties, cytotoxicity, and antibacterial activity, along with the combined effects of composites and electrical stimulation (ES) in a rat model of wound healing.

Results: Application of the PLGA/GO composites to full-thickness wounds confirmed their advantageous biological properties, as evident from the observed improvements in wound-specific mechanical properties, biocompatibility, and antibacterial activity. Additionally, we found that the combination of composites and ES improved composite-mediated cell survival and accelerated wound healing in vivo by promoting neovascularization and the formation of type I collagen.

Conclusion: These results demonstrated that combined treatment with the PLGA/GO composite and ES promoted vascularization and epidermal remodeling and accelerated wound healing in rats, thereby suggesting the efficacy of PLGA/GO+ES for broad applications associated with wound repair.

Keywords: wound repair, graphene oxide, electrical stimulation, tissue engineering, PLGA

Introduction

The skin is the largest organ in the human body and exhibits important physiological functions, such as protection and perception of temperature and pressure.[1] Severe trauma and certain diseases can cause open wounds in the skin and interfere with its normal structure and function. Because there is a lack of effective interventions, large skin defects can become life threatening;[2] And the USA spends $25 billion a year on wound healing for 6.5 million people. [3]Given the health and economic impact of wound healing, there is a need for wound healing therapy that promotes rapid healing and prevents associated infections

Electrical stimulation (ES) of tissues and cells can improve the biological functions of the heart, nerves, bones, and muscles.[4–6] Additionally, it is possible to regulate physiological functions, such as molecular transport, signal transduction, and embryonic development, via an external electrical field by regulating electric force and potential, K^+, Na^+, $Ca,^{2+}$ Cl^- levels in the body, and proteins present on the cell membrane.[7] Moreover, in vitro and in vivo experiments show that ES can alter the

Correspondence: Guoqing Zhao; Chuan Fu
Department of Anesthesiology, China-Japan Union Hospital of Jilin University, Changchun 130033, People's Republic of China
Tel +86 1 350 088 6187;
+86 1 575 430 6089
Fax +86 04 318 499 5299
Email guoqingzhao1965@163.com;
fuchuan2015@163.com

submit your manuscript | www.dovepress.com
DovePress
http://doi.org/10.2147/IJN.S216365

intrinsic current of the wound, downregulate nuclear factor-kappaB (NF-κB) signaling, affect cytokine expression, increase the proliferation and migration of endothelial cells, and improve wound healing.[8] In association with appropriate conductive biomaterials, ES can also improve the efficiency and mechanical effects of the electrical field and increase ion currents to regulate cell growth and differentiation.[9]

Conductive polymer materials are widely used in nerve regeneration and bone repair and are capable of controlling the growth of cells and tissues by promoting cell proliferation, simulating electronic or ionic conductivity, and medicating the flow of currents.[4,10–13] In addition to commonly used conductive polymer materials, such as polypyrrole, polyaniline, and metal nanowires, carbon-matrix materials are widely used owing to their good biocompatibility and biofunctionality.[6] Graphene oxide (GO) is an oxidized form of graphene with single-atomic layers that exhibit excellent conductivity and high chemical stability.[14] GO exists as a two-dimensional lattice comprising a unique monolayer of sp^2- and sp^3-hybridized carbon atoms. Previous studies confirmed the ability of GO to promote cell proliferation and adhesion,[15] and that conductive polymer materials containing GO can strengthen the ES, thereby accelerating wound healing.[16,17] Additionally,GO mediates the formation of extracellular superoxide compounds that can inhibit bacterial activity and reduce the risk of infection.[18] Moreover, dispersed GO nanoparticles exhibit low viscosity and cytotoxicity at high concentrations, thereby making them good candidates for local administration. The dispersed nanoparticles can also be converted into membrane materials to prolong their residence time on the skin surface and prevent biotoxicity.[19] To this end, we previously used a biodegradable copolymer,such as chitosan, PLGA, and collagen, as polymeric matrix to act as a binder for GO while manufacturing composites and produce new biomaterials with various biofunctions.[20] Poly(lactic-co-glycolic acid) (PLGA) is a biodegradable polyester copolymer composed of lactic acid and glycolic acid monomers,[21] and has the advantages of good biodegradability, mechanical properties,low immunogenicity and adjustable degradation rate, etc., which has attracted wide attention of people and can be used as the matrix material of GO.[22]

In this study, PLGA/GO composites were prepared using a blending method, and the physicochemical properties of the PLGA/GO composites were fully characterized by scanning electron microscopy (SEM), contact-angle measurements, and a material-testing machine. We investigated the effects of PLGA/CO composites combined with ES on wound repair, as well as the effect on the levels of proteins associated with cell proliferation and adhesion and tissue repair. Furthermore, we assessed the positive effects of PLGA/GO conductive composites and ES on wound healing in a rat model of full-thickness skin defects.

Materials and methods

Materials, cells, and animals

The reagents used in this study included the following: PLGA (LA:GA, 75:25; 130 kDa; Changchun Institute of Applied Chemistry, Chinese Academy of Sciences, Beijing, China); GO (thickness, 0.55–1.2 nm; diameter, 0.5–3.0 μm; Chengdu Organic Chemicals Co., Ltd., Chinese Academy of Sciences); trichloromethane (analytically pure; Aladdin Reagent Co., Ltd., Shanghai, China); type I collagen primary antibody; a fluorescein isothiocyanate (FITC)-conjugated fluorescent secondary antibody; a Cy5-conjugated fluorescent secondary antibody, a Cy3-conjugated fluorescent secondary antibody; 4,6-diamino-2-phenylindole (DAPI; Sigma-Aldrich, St. Louis, MO, USA); Dulbecco's modified Eagle medium (DMEM) and fetal bovine serum (Life Technologies, Carlsbad, CA, USA); penicillin and streptomycin (North China Pharmaceutical, China); trypsin, hematoxylin and eosin (H&E), and Masson trichrome staining kits (Solarbio, Beijing, China); methylthiazoletetrazolium (MTT; Gibco, Grand Island, NY, USA); and self-made phosphate buffered solution (PBS).

Adult female Sprague–Dawley rats (n=48; 10–12-weeks old; 200–250 g) were provided by the Animal Experimental Center of Jilin University [animal license No. SCXK (Ji) 20110004] and housed in a standard animal room (22 °C) administered by the same breeder, with pellet food and water available *ad libitum*.

Balb/c3T3 cells (Shanghai Institute of Biological Sciences, Chinese Academy of Sciences) were cultured in DMEM containing 10% serum concentrations of penicillin and streptomycin at 37 °C and 5% CO_2, and the medium was changed every 2 days. Upon reaching 80% confluence, cells were used for subsequent experiments.

Preparing PLGA/GO composites

We prepared PLGA/GO electroactive nanocomposites using a solution-volatilization method, as follows. We dissolved GO and PLGA in chloroform to prepare a 5% chloroform solution before incorporating different mass concentrations of GO (0.5%, 1%, 2%, and 5%) into the

PLGA, followed by magnetic stirring and mixing the solution thoroughly by ultrasonic vibration. The composites were prepared at a ratio of 6 cm^2/mL,[23] with some spread using a siliconized circular coverslip for cell experiments and material characterization, and others placed into a glass culture dish for animal experiments, followed by natural drying and peeling. The slides and composites were dried in vacuum for 48 h.

Composite characterization

Structure

Samples were cut into small pieces (3×3 mm) and sprayed with gold, after which the surface morphology of the PLGA/GO composites at different concentrations was observed at 20 kV by SEM (XL30 ESEM-FEG; FEI; Thermo Fisher Scientific, Waltham, MA, USA).

Hydrophilicity

An instrument capable of measuring the optical contact angle (DSA100; Kruss GmbH, Hamburg, Germany) was used to measure the static water-contact angle to assess the surface hydrophilicity of the PLGA/GO composites at different concentrations. We removed some of the composites and adhered them to a slide using double-sided tape, followed by application of 2 μL of deionized water directly to the sample surface at room temperature. Because the measuring instrument includes a camera, we photographed the droplets and measured the contact angle.

Mechanical properties

A universal mechanical testing machine (Instron 1121; Instron, Wycombe, UK) was used to test a nanofiber-matrix sample (10×30 mm) with two ends clamped onto the testing machine. The upper end was lifted at a constant tensile rate until the sample was completely broken, at which time the tensile stress was recorded.

Determination of antibacterial activity

After disinfection, PLGA/GO composites at different concentration on the coverslip were placed into a culture dish, with a blank culture dish used as a control. *Staphylococcus aureus* or *Escherichia coli* Luria-Bertani (LB) solution (50 μL; 1×10^7/mL) was added to each culture dish, followed by a 3-h incubation at 37 °C. The samples were rinsed with PBS three times, recovered, and concentrated using the recovered bacterial solution. The resuspended dilution (30 μL) was spread onto an LB agar plate and incubated at 37 °C overnight. Colonies were counted after overnight incubation, and the inhibition rates of the composites at different concentrations were calculated using the following formula: inhibition rate (%) = (number of colonies in the control group − number of colonies in the experimental group)/number of colonies in the control group ×100%.

Cytological testing

Effects of different GO concentrations on cell viability

The composites were immersed in 75% alcohol for 30 min, rinsed three times with PBS, and placed in a 24-well plate for overnight incubation at 37 °C. Balb/c3T3 cells were then seeded at a density of 2×10^4 cells/well, and the medium was changed every 2 days. On days 1, 3, and 7, MTT assays were performed to determine cell survival on the surface of the PLGA/GO composites at different concentrations. MTT/PBS solution (5 mg/mL; 100 μL) was added to each well and incubated at 37 °C for 4 h, followed by removal of the medium and addition of acidified isopropanol (75 μL/well). The absorbance of the solution was measured at a wavelength of 540 nm using ultraviolet-visible spectroscopy (UV300; UNICAM; Thermo Fisher Scientific), and based on these results, we chose the optimal GO concentration for subsequent experiments.

Effects of ES at different frequencies on cell viability

Balb/c3T3 cells were seeded into 24-well plates at 2×10^4 cells/well for 24 h. The electrodes were immersed in 75% ethanol for 10 min, washed with sterile PBS, and irradiated with ultraviolet light overnight. A pair of L-shaped platinum electrodes with an interval of 10 mm was placed on the cover of the culture plate, and a function signal generator was connected to the electrodes through an alligator clip and copper wire to create a signal source. Balb/c3T3 cells were exposed to 100 mV ES for 1 h daily at a frequency ranging from 10 Hz to 1000 Hz. After 1, 3, and 7 days of ES, MTT assays were performed to detect the effect of ES at different frequencies on cell survival. Based on these results, the optimal frequency was selected for subsequent experiments. All tests were performed 24 h after the final exposure.

Effects of PLGA/GO composites and ES on cell survival and adhesion

MTT assays and immunofluorescence staining were used to evaluate the effects of PLGA/GO composites and ES on the survival and adhesion of Balb/c3T3 cells. Four groups were used for experimental evaluation: PLGA, PLGA+ES, PLGA/GO, and PLGA/GO+ES. Cells (2×10^4) were added to each well of a 24-well plate, and survival was determined in each

group by MTT assay on days 1, 3, and 7. To evaluate cell spreading and adhesion, cells were added to a separate 24-well plate at the same density, and after a 3-day culture, the samples were fixed in 4% paraformaldehyde for 15 min and rinsed three times with PBS. FITC (green) and DAPI (blue) were used to label the cytoskeleton and nucleus as follows. Samples were mounted in blocking solution (0.1% Triton-X 100+10% bovine serum albumin) for 30 min at room temperature. Prepared FITC solution was applied at room temperature in a wet box for 2 h, followed by three washes with PBS containing Tween-20 (PBST). The samples were developed using DAPI for 1 min, rinsed three times with PBST, and observed under a fluorescence microscope (TE2000-U; Nikon, Tokyo, Japan).

Effects of PLGA/GO composites and ES on gene expression and protein levels

The expression of genes related to tissue repair in Balb/c3T3 cells was quantitatively analyzed in the four groups following a 7-day culture. Total RNA was extracted, the levels were determined by nano-titration (Tecan M200; Tecan Life Sciences, Männedorf, Switzerland), and reversely transcribed to cDNA. Primers targeting *vascular endothelial growth factor* (*VEGF*) and *type 1 collagen* (*COL-1*) were designed using sequences from GenBank (https://www.ncbi.nlm.nih.gov/genbank/). The primer sequences are shown in Table 1.

COL-1 was quantitatively detected by immunofluorescence analysis. Cell grouping and culture were the performed as described, and after a 3-day culture, cells were fixed in 4% paraformaldehyde for 15 min, washed with PBS three times, and mounted at room temperature for 30 min. The cells were treated with the COL-1 primary antibody and bathed in the wet box at 4 °C overnight, followed by three washes with PBST. A Cy5-conjugated secondary antibody was then applied at room temperature for 2 h, followed by three washes with PBST. The cells were then developed using DAPI for 1 min, washed with PBST three times, and observed under a fluorescence microscope (TE2000-U; Nikon).

Animal experiments

Effects of PLGA/GO composites and ES on the wound-healing rate

All protocols were conducted in accordance with the guidelines for the review and approval of the Animal Care and Use Committee of Jilin University, China (approval number: 2018–191) on June 10, 2018 and were performed in accordance with the Guide for the Care and Use of Laboratory Animals, adopted and published by the US National Institutes of Health. Precautions were taken to reduce the pain (see anes- thesia procedure below) and the number of rats used in each experiment.Three days prior to the experiment, the back hair of rats was removed using depilatory cream (Veet, Hubei Province, China). The PLGA/GO and PLGA were soaked in 75% alcohol for 24 h prior to the experiment and disinfected with ultraviolet light. After anesthesia, the back skin of the rats was disinfected using iodine, a full-thickness skin defect of 1-cm diameter was made on the back based on a plastic model prepared in advance, and the wound was photographed. Rats (n=25) were randomly divided into five groups: control, PLGA, PLGA/GO, PLGA+ES, and PLGA/GO+ES (n=5/group) Each skin defect was dressed with the corresponding composite, covered with gauze, and fixed with nylon thread. ES was applied to rats in the two ES groups daily for 5 min.[24] On postoperative days 3, 6, 9, and 12, the dressing was changed, the wound was photographed with the digital camera in an iPhone (Apple Corp., Cupertino, CA, USA), and measured with an image analysis software (ImageJ; National Institutes of Health, Bethesda, MD, USA). Wound-healing rate was determined according to the following formula: wound healing rate = $[(A_0 - A_t)/A_0] \times 100\%$, where A_0 is the initial area of the wound at time zero (t=0), and A_t is the wound area at the measurement time.

Histopathologic staining

All rats were euthanized on day 12 after injury, and the wound and surrounding skin were completely removed and equally cut into two parts, with one part used for immunofluorescence staining. Fresh tissue blocks were

Table 1 List of genes and primer sequences

Gene Annotation	Forward primer sequence	Reverse primer sequence
COL-1	CGCTGGCAAGAATGGCGATC	ATGCCTCTGTCACCTTGTTCG
VEGF	CCTTGCCTTGCTGCTCTACC	AGGTTTGATCCGCATGATCTG
GAPDH	TGAACTAACACAGAGGAGGATCAG	GCTTAGGGCATGAGCTTGAC

fixed in 10% formalin, embedded in paraffin, and cut into tissue slices (5 μm). At least six serial slices were taken near the center of the wound, with each slice including both normal tissue and wound tissue taken at the wound edge. The slices were stained with Masson and H&E, and histological changes were observed under an optical microscope (CTR600; Leica, Wetzlar, Germany)).

Immunofluorescence staining

The remaining fresh tissue blocks were embedded and cut into 10 μm frozen-tissue slices using a cryotome, followed by antigen retrieval and blocking. COL-1 (1:300) and CD31 (1:400) primary antibodies were used in the wet box at 4 °C overnight, and corresponding Cy5- and Cy3-conjugated secondary antibodies (1:500) were applied at room temperature for 2 h. The slices were rinsed with PBST and mounted with DAPI, after which COL-1 levels were determined using Image-Pro software (Media Cybernetics, Cambridge, UK). Five regions (50×50 μm each) were randomly obtained to measure the average fluorescence intensity for quantitative analysis. CD31-labeled neovascularization was observed under a fluorescence microscope (TE2000-U; Nikon).

Statistical analysis

Data were statistically analyzed using Origin 8.0 software (OriginLab, Northampton, MA, USA), and dose data were expressed as the mean ± standard deviation. Statistical differences were assessed using one-way analysis of variance and a post hoc test. A $P<0.05$ was considered statistically significant.

Results and discussion

As shown in Figure 1, we prepared two types of composites for characterization analysis, cell experiments, and animal experiments and created a full-thickness skin-defect rat model to verify the effects of composites alone or in combination with ES on wound treatment.

Surface topography of the composites

We observed the surface morphologies of PLGA and PLGA/GO composites at mass concentrations of 0.5%, 1%, 2%, and 5% by SEM. As shown in Figure S1, the surface of the pure PLGA composites was smooth and flat, whereas that of the PLGA/GO composite was rough and wrinkled. Moreover, the surface roughness of the PLGA/GO composite increased along with increasing GO concentration, with some nanoparticles aggregating to form large particles. Previous studies report that increased roughness increases the surface adsorption of vitronectin and fibronectin and promotes the growth of surface cells.[25,26] Therefore, these results suggested that GO incorporation not only changed composite surface morphology but also improved its biocompatibility.

Composite hydrophilicity

Previous studies show that cell adhesion and proliferation can be improved by increasing the hydrophilicity of biological

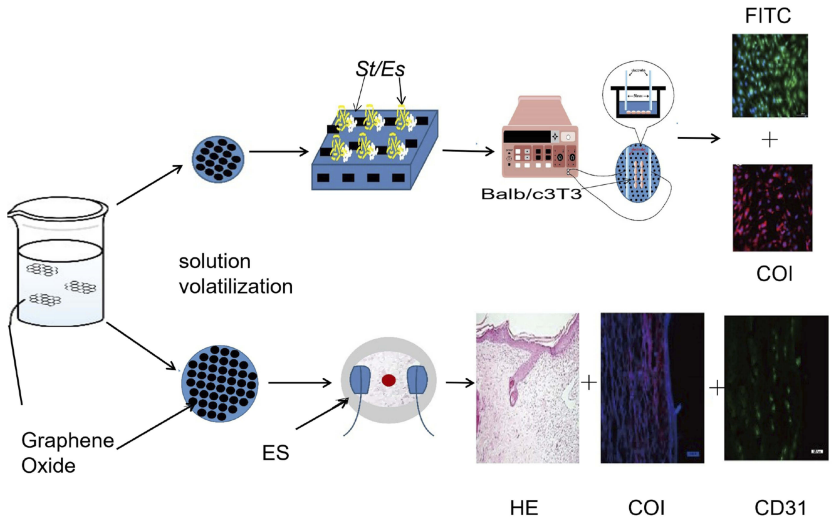

Figure 1 Preparation of the PLGA/GO composite and its application for wound treatment.
Abbreviations: ES, electrical stimulation; St, *Staphylococcus aureus*; Es, *Escherichia coli*.

materials. As shown in Figure 2A, GO incorporation enhanced PLGA hydrophilicity, with surface hydrophilicity being positively correlated with GO concentration. PLGA/GO composite hydrophilicity is dependent upon the existence of hydrophilic groups, such as –OH, C-O-C, and –COOH, on the GO surface. Our results showed that compared with pure PLGA, the surface contact angle of the 0.5% PLGA/GO composites was slightly reduced, whereas those of the 1%, 2%, and 5% PLGA/GO were significantly reduced (P<0.05).

Increased GO concentration clearly improved the hydrophilicity of the composites, and this phenomenon may be ascribed to the presence of hydrophilic –OH, C–O–C, and –COOH groups on GO surface. Furthermore, GO can affect composite hydrophilicity by changing surface nanomorphology and topography,[27] which is likely another explanation for the improved hydrophilicity of the composites. Moreover, the hydrophilicity of the scaffold surface enhanced cellular behavior, including initial attachment, proliferation, and differentiation; therefore, the PLGA/GO composites provided a suitable microenvironment for cell attachment and proliferation based on the presence of a more hydrophilic surface relative to other matrices.

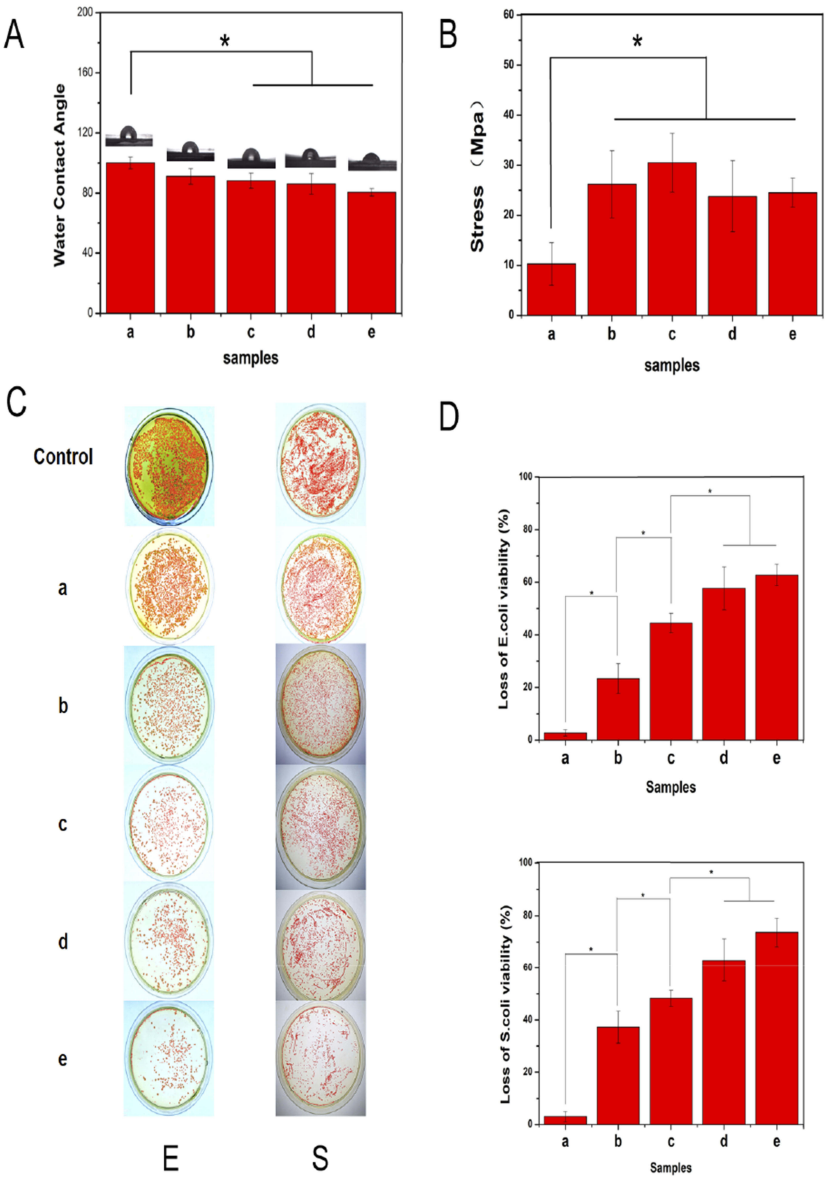

Figure 2 Characteristics of the PLGA/GO composites. (**A**) Water contact angle and (**B**) tensile strength of the PLGA incorporated with different concentrations of GO. (a) PLGA, (b) PLGA/GO composites (0.5%), (c) PLGA/GO composites (1 wt%), (d) PLGA/GO composites (2 wt%), and (e) PLGA/GO composites (5 wt%). *P<0.05 (n=3).(**C**) Photographs of bacterial colonies formed by *E. coli* and *S. aureus* cells treated with (a) PLGA, (b) PLGA/GO composites (0.5%), (c) PLGA/GO composites (1 wt%), (d) PLGA/GO composites (2 wt%), and (e) PLGA/GO composites (5 wt%). (**D**) Loss of *E. coli* and (C) *S. aureus* cell viability. *P<0.05 (n=3).

Mechanical properties of the composites

Tissue scaffolds must have excellent mechanical properties, and adequate strength and ductility allow composites to be better adapted to the extension or flexion caused by morphological and structural changes during skin healing.[28] Moreover, previous studies indicate that the mechanical performance of the composite affects cell growth and differentiation.[29,30] A study by Wuhan University of Technology shows that,biomaterials with sufficient mechanical strength are beneficial to the adhesion and migration of cells in vitro.[31] In addition, previous animal studies have found that the good mechanical properties of biomaterials contribute to the realization of shape memory and are suitable for wound healing combined with skin.[32] Although the mechanical properties of PLGA cannot meet the requirements of tissue engineering, GO incorporation into the PLAG can effectively improve its mechanical and biological properties. Figure 2B shows the tensile strength of different composites. The results indicated that adding a small amount of GO significantly improved the mechanical properties of the composites, with tensile strengths of 2% and 5% PLGA/GO composites decreasing slightly but still remaining superior to that of the PLGA ($P<0.05$). The incorporation of GO at high concentrations might cause decreased tensile strength owing to agglomeration or re-crushing of the GO nanoparticles via hydrogen bonding or electrostatic interactions. Therefore, GO nanoparticles cannot uniformly distribute in the PLGA.

Antibacterial activity of the composites

Damaged skin exhibits loss of the barrier protecting the host from pathogens. Moreover, exudate and proteins from ischemic necrotic tissue can cause bacterial infection, delay wound healing, and increase exudation and improper collagen deposition.[33] Therefore, excellent antibacterial properties are important characteristics of high-quality wound dressings; however, pure PLGA polymers have no antibacterial properties. By contrast, GO exhibits spectral antibacterial properties against Gram-positive and -negative bacteria and does not trigger drug resistance.[34] This is mainly because of the ability of nano-scale GO to generate superoxide in the extracellular space of bacteria in order to exert chemical damage. Additionally, the high degree of roughness on the GO surface can mechanically damage the bacterial cell membrane, thereby exerting antibacterial activity.[18,35] Furthermore, the PLGA/GO composites act as conductive polymers and can cause a variety of biological effects leading to bacterial cell death facilitated by electron transport between bacterial cells.[36,37]

In the present study, we assessed the antibacterial effects of PLGA/GO composites on the common skin pathogens *E. coli* and *S. aureus*. As shown in Figure 2C, the pure PLGA showed almost no antibacterial activity, whereas addition of GO increased this activity against both pathogens, with the inhibition rate against *S. aureus* being higher than that against *E. coli*. Additionally, the antibacterial effect of the PLGA/GO composites increased along with increase in GO concentration, although there was no significant increase in antibacterial activity between the 2% PLGA/GO and the 5% PLGA/GO composites.

Effects of composites harboring different GO concentrations on cell survival

Mouse fibroblasts are commonly used in wound-repair studies owing to their important role in wound healing, including in the formation of granulated tissues that fill the wound and differentiation into myofibroblasts involved in wound contraction.[38] Fibroblasts secrete growth factors, such as VEGF, platelet-derived growth factor, and basic fibroblast growth factor, and promote formation of the extracellular matrix to increase the neovascularization ability of endothelial cells.[39–43] Figure S2 shows the effect of different GO concentrations on cell survival. After a 1-day culture, only the 1% PLGA/GO composites showed a significant effect on cell survival when compared with the pure PLGA composite, whereas after 3 days, 2% PLGA/GO composites showed the highest survival ($P<0.05$). After a 7-day culture, the number of surviving cells on the PLGA/GO composites was significantly higher than that on the pure PLGA, although we observed a higher number of surviving cells on the 2% PLGA/GO composites than on the 5% PLGA/GO composites.

GO influences cell survival owing to its optimal electrical activity, which can induce chemical and energy exchange between cells and the surrounding environment and promote cell growth and proliferation by transmitting electrical signals to attached cells.[44–46] Additionally, SEM results and contact-angle measurements showed that the PLGA/CO composites displayed increased surface roughness and hydrophilicity, which also promote cell proliferation. However, compared with the 2% composite, the 5% composite was cytotoxic, thereby inhibiting cell proliferation, which is consistent with results reported in previous studies suggesting that GO nanoparticles exhibit low

viscosity and cytotoxicity at high concentrations.[19,46,47] As a degradable organic polymer, PLGA can reduce the GO-contact area with cells and tissues in order to avoid release of excessive amounts of GO, thereby avoiding cytotoxic effects while retaining the antibacterial and value-added effects of the PLGA/GO composite. Based on our results, we used the 2% PLGA/GO composite for subsequent experiments.

Effect of different ES frequencies on cell survival

To determine the optimal ES frequency for subsequent experiments, we examined the effect of different ES frequencies on cell proliferation. As shown in Figure S2B, on culture day 1, cell viability at each ES frequency was higher than that in the control group (0 Hz), although there was no statistical difference between groups. Additionally, ES showed an increasing effect on cell survival along with prolonged culture time, with the highest cell-survival rate observed in the 500-Hz group on day 7 ($P<0.05$, 500 Hz vs 100 Hz). Previous studies reported that ES at a constant frequency promotes the growth and migration of dermal fibroblasts through the transforming growth factor-β1/extracellular-signal-regulated kinase (ERK)/NF-κB signaling pathway, secretion of cytokines and growth factors, and activation of cellular pathways involved in cell proliferation.[48,49] Based on our results, we used 500 Hz ES for subsequent experiments.

Effect of PLGA/GO composites and ES on cell proliferation and adhesion

To observe the effects of PLGA/GO and ES on cell viability, we determined changes in cell survival by MTT assays on days 1, 3, and 7 under different culture conditions (Figure 3.1A). On culture day 1, the PLGA/GO composite did not show clear effects on cell survival; however, on culture day 3, both the PLGA/GO composite and ES, respectively, increased the number of surviving fibroblasts significantly, and on culture day 7, we observed further increases in the number of surviving fibroblasts in the PLGA/GO, PLGA+ES, and PLGA/GO+ES groups relative to that in the PLGA and control groups. Quantitative analysis indicated that the PLGA/GO +ES group showed a synergistic advantage over single-factor intervention.

We then evaluated the morphological characteristics of Balb/c3T3 cells grown on different composites by immunofluorescence staining (Figure 3.1B). We observed a larger number of cells in the PLGA/GO, PLGA+ES, and PLGA/GO+ES groups relative to that in the PLGA group, which was consistent with the results of MTT assays. Additionally, cells in these intervention groups exhibited better cytoskeletal characteristics and spreading activity, indicating that ES along with the PLGA/GO composites was beneficial to both cell survival and adhesion. This can be explained by the hydrophilicity of the PLGA/GO composite according to the presence of –COOH and –OH functional groups. Moreover, as an electroactive nanomaterial, GO can improve the endogenous bioelectricity of cells, with the local electric field generated by ES being capable of mediating the diffusion of extracellular matrix proteins and their translocation to the cell surface to promote cell adhesion and diffusion.[50,51] These results confirmed that the unique physicochemical properties of GO promoted cell proliferation and adhesion and regulated the effects of ES on enhancing the physiological function of cells.

Effect of PLGA/GO composites with ES on the expression of genes related to tissue repair

Fibroblasts fill and astringe wounds and promote angiogenesis during skin healing accompanied by changes in the expression of associated genes, including *COL-1* and *VEGF*. COL-1 affects skin structure, function, and texture characteristics,and VEGF is a major growth factor that promotes neovascularization by endothelial cells.[38,39] As shown in Figure 3.2A, *VEGF* expression in the PLGA/GO group did not differ significantly from that in the PLGA group; however, these levels were significantly enhanced in the ES and PLGA/GO+ES groups, suggesting that the PLGA/GO composite enhanced ES-mediated vascularization by fibroblasts. Although the mechanism by which ES increases *VEGF* expression remains unclear, this activity has been confirmed in previous studies involving the heart, bone, cartilage, and muscle.[52,53] Furthermore, we found similar results associated with *COL-1* expression, implying a synergistic effect of ES and PLAG/GO, which resulted in the highest levels of gene expression in the PLGA/GO+ES group.

To evaluate the effects of different interventions on tissue repair, we employed immunofluorescence staining to observe changes in COL-1 protein levels in different groups. As shown in Figure 3.2B, changes in fluorescence associated with COL-1 levels confirmed quantitative

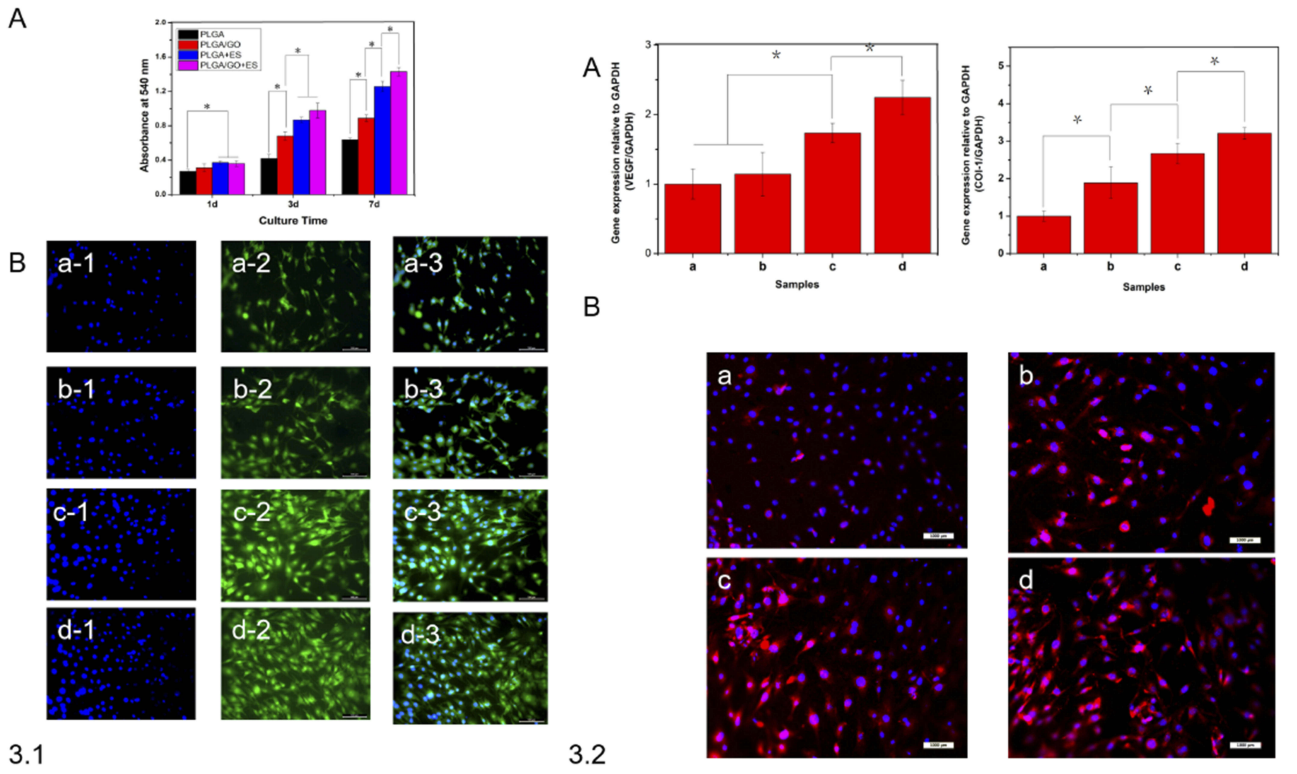

Figure 3 3.1. PLGA/GO-mediated changes in morphology. (**A**) Cell viability according to MTT assay (absorbance at 540 nm) at each time point and under different culture conditions. *P<0.05 (n=3). (**B**) Morphology of Balb/c3T3 cells cultured under different conditions for 3 days. Staining of the cytoskeleton (green) and nucleus (blue). Scale bars, 100 μm. 3.2. qRT-PCR analysis of genes related to tissue repair. (**A**) Measurement of VEGF and COL-I levels following Balb/c3T3 cell culture for 7 days under different conditions. (a) PLGA biofilm, (b) PLGA/GO composites (2 wt%), (c) ES, and (d) PLGA/GO composites (2 wt%) + ES (n=4 replicates). *P<0.05 (n=4) (**B**) Immunofluorescence images of COL-I protein under different culture conditions. (a) PLGA biofilm, (b) PLGA/GO composites (2 wt%), (c) ES, and (d) PLGA/GO composites (2 wt%) + ES. Scale bars, 100 μm.

reverse transcription polymerase chain reaction (qRT-PCR) results and suggested that PLGA/GO+ES was most effective at promoting the expression and translation of molecules related to tissue repair.

In vivo changes in the wound-healing rate

Figure 4A shows the macroscopic appearance of the wound at different time points post-operation, with differences in healing rate between groups being the most obvious on day 6 post-injury.As shown in Figure 4B, the healing rates in the PLGA, control, PLGA/GO, and PLGA +ES groups increased gradually (P<0.05 between groups) and this trend continued until sacrifice on day 12 (P>0.05, PLGA+ES vs PLGA/GO+ES; and PLGA vs control). Given the beneficial characteristics of GO, its incorporation with the PLGA biofilm exhibits positive effects on in vivo wound healing, based on the significantly higher rate relative to that observed in the PLGA and control groups. Importantly, the PLGA/GO composite promoted tissue repair via exogenous ES, with the wound-healing rate observed in the PLGA/GO+ES group consistently exceeding that of other groups.

Histologic analysis

Re-epithelialization and collagen deposition/alignment are essential for wound healing.[54] H&E and Masson's trichrome staining of the wound and surrounding tissues showed larger wounds accompanied by a thicker epithelium and a clear subepidermal space in the control and PLGA groups (Figure 5A, blue area). By contrast, both the PLGA/GO and the PLGA/GO+ES groups displayed decreases in inflammatory tissue accompanied by scar formation on the lesion surface (Figure 5A, purple arrow) and capillary proliferation. Additionally, the PLGA/GO group displayed thinning epithelial tissue and new epidermal tissues covering both ends of the lesion. Similarly, in the PLGA+ES and PLGA/GO+ES groups, the epidermis on the wound surface was thinned, and new capillary capillaries (Figure 5A, yellow arrow) were visible in the granulated tissue of the damaged area, with optimal therapeutic results observed in the PLGA+ES and PLGA/GO+ES groups.

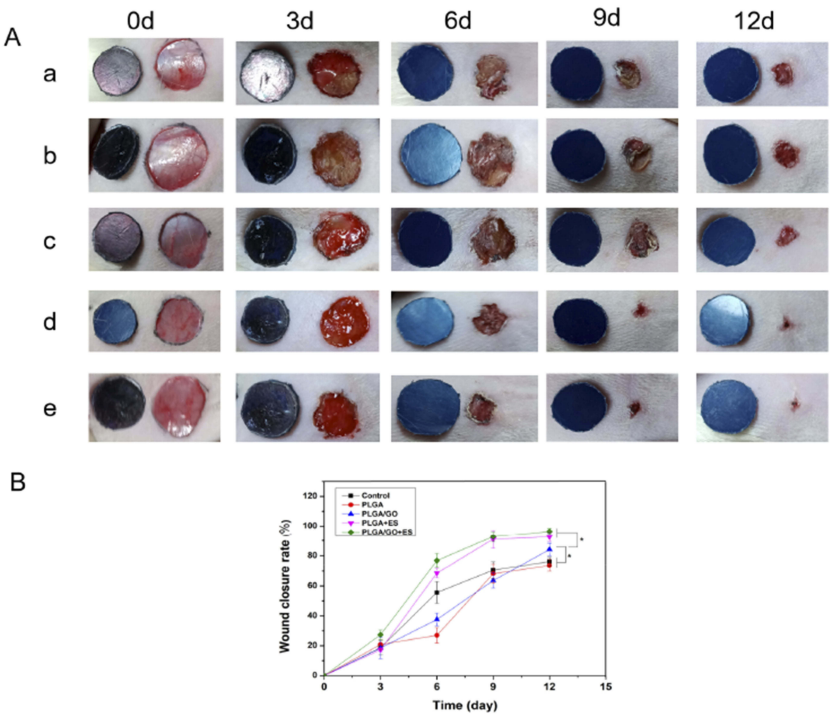

Figure 4 The differential effects of PLGA/GO composites and ES on wound healing. (**A**) Representative macroscopic appearance of wounds. (a) Control, (b) PLGA, (c) PLGA/GO composites (2 wt%), (d) PLGA + ES, and (e) PLGA/GO composites (2 wt%) + ES. (**B**) Wound-healing curves. *P<0.05 (n=5).

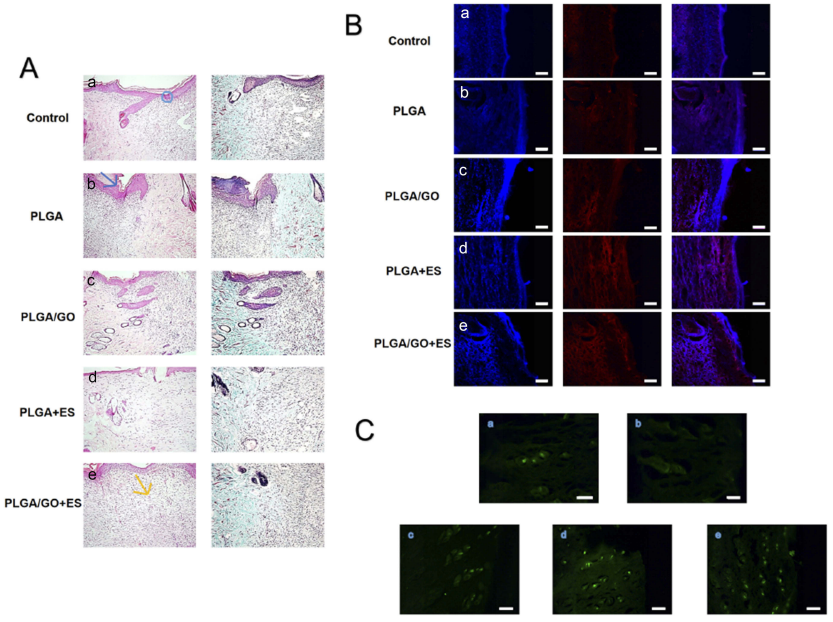

Figure 5 Differential effects of PLGA/GO composites and ES on tissue structure of wounds at 12 days. (**A**) Histological results. (a) Control, (b) PLGA biofilm, (c) PLGA/GO composites (2 wt%), (d) PLGA+ES, and (e) PLGA/GO composites (2 wt%) + ES. Magnification, 100×. Blue circle indicates subepidermal space, blue arrow indicates scar formation, yellow arrow indicates new capillary capillarie. (**B**) Immunofluorescence images of COL-1 levels in the wound-healing region at 12 days after different treatments. (a) Control, (b) PLGA biofilm, (c) PLGA/GO composites (2 wt%), and (d) PLGA+ES, and (e) PLGA/GO composites (2 wt%) + ES. Scale bars, 500 μm. (**C**) Immunohistochemical staining and quantification of CD31-positive microvessels in the wound-healing region at 12 days after different treatments. (a) Control, (b) PLGA, (c) PLGA/GO composites (2 wt%), and (d) PLGA+ES, and (e) PLGA/GO composites (2 wt%) + ES. Scale bars, 100 μm.

Epithelial repair involves a transition from epithelial thickening to thinning owing to increased proliferation and/or delayed differentiation of cells during the early stage of injury repair, as well as an increase in the number of keratinocytes. Subsequently, the differentiation of the stratum corneum accelerates into the epidermis until skin thickness is recovered.[41] In the present study, we observed denser neoplastic tissues in the PLGA/GO+ES group, confirming that the combination of the PLGA/GO composite and applications of an ES promoted cell proliferation and adhesion during wound healing.

Analysis of changes in collagen content at the injury site

COL-1 is the main structural component of the dermis and exists at high levels in the dermis of normal skin. During the early stage of injury, epidermal tissue is in the proliferative stage and exhibits elevated expression of *COL-3* and attenuated expression of *COL-1* in granulated tissue, until epidermal remodeling, during which *COL-1* expression increases and gradually exceeds that of *COL-3*.[55] In the present study, we observed improved epithelial remodeling in the PLGA+ES and PLGA/GO+ES groups relative to that in other groups and accompanied by elevated *COL-1* expression (Figure 5B). This was mainly due to ES effectively promoting fibroblast proliferation (Figure 3.1) and increasing collagen production. Additionally, the PLGA/GO group displayed higher *COL-1* expression than that in the PLGA and control groups, possibly due to the antibacterial properties of GO (Figure 2C). Moreover, GO inhibited bacterial growth in the wound site and accelerated wound healing and collagen deposition. These results indicated that the PLGA/GO composite exhibited excellent physical properties, including mechanical strength, hydrophilicity (Figure 2), and protein adsorption, thereby creating a better living environment for cells and promoting tissue healing.

Analysis of vascularization

New blood vessels provide micronutrients, amino acids, and oxygen to damaged skin, which are essential for healing, epithelialization, and fibrosis.[56] In the present study, we used the endothelial-cell-specific protein marker CD31 as a marker of neovascularization around the wound. As shown in Figure 5C, we observed a significantly higher number of new blood vessels in the PLGA/GO group relative to that in the control and PLGA groups, with further increases observed following ES intervention. Given the synergy observed between the PLGA/GO composite and ES, we found that the number of new blood vessels in the PLGA/GO+ES group was even higher than that in the PLGA+ES group. This was consistent with the results of cell experiments (Figure 3.2) and those reported in previous studies.[57–59]

These findings can be explained through the ability of ES to regulate mitogen-activated protein kinase/ERK signaling in vascular endothelial cells, which increases VEGF levels and promotes angiogenesis. Moreover, studies show that electroactive dressings can affect the physiological functions of surrounding cells through the Ca^{2+}/calmodulin pathway to enhance the biological effects of exogenous ES.[46,60,61]

The treatment of large-area skin defects caused by severe burns and trauma remains a challenge in wound treatment. Invasive treatments, such as skin grafting, cannot meet clinical needs owing to limited donor sources and the presence of significant secondary damage. With advances in tissue-engineering technology, the use of artificial dressings made of degradable polymers has attracted increasing attention for their ability to promote the repair of large-area skin defects. The ideal tissue-engineered skin dressing should exhibit good histocompatibility, mechanical strength, and antibacterial and electrophysical properties in order to provide an ideal environment for seed-cell growth and proliferation and promote skin self-repair. In the present study, we incorporated GO into biodegradable PLGA in order to improve the biocompatibility and tissue-repair ability of the PLGA dressing, as well as to optimize the physical and chemical properties of the composite material. Following the addition of GO, PLGA exhibited an ability to preclude GO release, which avoided associated cytotoxic effects while retaining the antibacterial and value-added effects of the PLGA/GO composite. SEM, mechanical, and contact-angle analyses of the PLGA/GO composite revealed that incorporation of the optimal GO concentration (2%) improved the mechanical strength and hydrophilicity of the composite, as well as increased the surface roughness to promote cell adhesion. Moreover, we found that the PLGA/GO composite exerted obvious antibacterial effects against *S. aureus* and *E. coli*.

To further enhance the physiological function of the PLGA/GO composite, we combined its application with ES based on insights from previous studies reporting its efficacy for enhancing the biological function of PLGA/GO composites,[7] especially in epidermal repair,[8] through

multiple signaling pathways. The effects of ES on electroactive biomaterials can accelerate the process of tissue repair, with our experimental results showing that ES increased the survival of Balb/c3T3 cells and upregulated mRNA and protein levels of VEGF and COL-1. Importantly, PLGA/GO and ES exhibited synergistic effects that promoted cell proliferation and upregulated levels of proteins associated with tissue repair. Furthermore, our in vivo findings in rats showed that PLGA/GO+ES promoted wound healing, accelerated epidermal remodeling, and facilitated neovascularization to the highest degree. Therefore, these results indicated that ES combined with the PLGA/GO composite represents a promising approach for epidermal repair and artificial skin preparation. Our future work will improve the biological characteristics of conductive composite dressings and their interaction with electrical fields in order to obtain an optimal dressing for tissue-engineering applications.

Conclusion

Here, we demonstrated the efficacy of PLGA/GO as a conductive composites with excellent mechanical properties, hydrophilicity, and antibacterial activity. The morphology and surface properties of the composite were efficacious for skin-tissue regeneration and worked synergistically with ES to improve cell adhesion and proliferation and promote the transcription of genes associated with tissue repair. Our results showed that combined treatment with the PLGA/GO composite and ES promoted vascularization and epidermal remodeling and accelerated wound healing in rats, confirmed according to improvements in gross appearance, histological observations, and immunofluorescence staining. These findings suggest the efficacy of PLGA/GO+ES for broad applications associated with epidermal repair.

Abbreviations

COL-1, type 1 collagen; DAPI, 4,6-diamino-2-phenylindole; DMEM, Dulbecco's modified Eagle medium; ERK, extracellular-signal-regulated kinase; ES, electrical stimulation; FITC, fluorescein isothiocyanate; GO, graphene oxide; H&E, hematoxylin and eosin; LB, lysogeny broth; MTT, methylthiazoletetrazolium; NF-κB, nuclear factor-kappaB; PBS, phosphate-buffered saline; PBST, PBS containing Tween-20; PLGA, poly(lactic-co-glycolic acid); SEM, scanning electron microscopy; VEGF, vascular endothelial growth factor.

Acknowledgment

This study was funded by Graduate Innovation Fund of Jilin University (No. 101832018C074).

Author contributions

G.Z. and C.F. were involved in experimental design and manuscript modification; D.Y. performed the experiments and data analysis and wrote the manuscript; K.L. performed the experiments and data analysis; and W.G. performed data analysis. All authors contributed to data analysis, drafting and revising the article, gave final approval of the version to be published, and agree to be accountable for all aspects of the work.

Disclosure

The authors report no conflicts of interest in this work.

References

1. Sheikholeslam M, Wright MEE, Jeschke MG, et al. Biomaterials for skin substitutes. *Adv Healthc Mater*. 2018;7(5).
2. Kheradvar SA, Nourmohammadi J, Tabesh H, et al. Starch nanoparticle as a vitamin E-TPGS carrier loaded in silk fibroin-poly (vinyl alcohol)-Aloe vera nanofibrous dressing. *Colloids Surf B*. 2018;166:9–16.
3. Li Q, Niu Y, Diao H, et al. In situ sequestration of endogenous PDGF-BB with an ECM-mimetic sponge for accelerated wound healing. *Biomaterials*. 2017;148:54–68.
4. Dong R, Zhao X, Guo B, et al. Biocompatible elastic conductive films significantly enhanced myogenic differentiation of myoblast for skeletal muscle regeneration. *Biomacromol*. 2017;18(9):2808–2819.
5. Fabbro A, Scaini D, León V, et al. Graphene-based interfaces do not alter target nerve cells. *J ACS Nano*. 2016;10(1):615–623.
6. Dvir T, Timko BP, Brigham MD, et al. Nanowired three-dimensional cardiac patches. *Nat Nanotechnol*. 2011;6(11):720–725.
7. Wang Y, Rouabhia M, Zhang Z. PPy-coated PET fabrics and electric pulse-stimulated fibroblasts. *J Mater Chem B*. 2013;1(31):3789–3796.
8. Ghafar-Zadeh E, Waldeisen JR, Lee LP. Engineered approaches to the stem cell microenvironment for cardiac tissue regeneration. *Lab Chip*. 2011;11(18):3031–3048.
9. Pesce M, Patruno A, Speranza L, Reale M. Extremely low frequency electromagnetic field and wound healing: implication of cytokines as biological mediators. *J Eur Cytokine Netw*. 2013;24(1):1–10.
10. Collazos-Castro JE, Polo JL, Hernández-Labrado GR. Bioelectrochemical control of neural cell development on conducting polymers. *J Bio Mater*. 2010;31(35):9244–9255.
11. Gilmore KJ, Kita M, Han Y, et al. Skeletal muscle cell proliferation and differentiation on polypyrrole substrates doped with extracellular matrix components. *Biomaterials*. 2009;30(29):5292–5304.
12. Aznar-Cervantes S, Pagán A, Martínez JG, et al. Electrospun silk fibroin scaffolds coated with reduced graphene promote neurite outgrowth of PC-12 cells under electrical stimulation. *Mater Sci Eng C Mater Biol Appl*. 2017;79(p):315–325.
13. Qi Z, Xia P, Pan S, et al. Combined treatment with electrical stimulation and insulin-like growth factor-1 promotes bone regeneration in vitro. *PLoS One*. 2018;13(5):e0197006.

14. Feng ZQ, Wang T, Zhao B, et al. Soft graphene nanofibers designed for the acceleration of nerve growth and development. *Adv Mater*. 2015;27(41):6462–6468.
15. Fu C, Sun B, Sun S, et al. Enhanced cell proliferation and osteogenic differentiation in electrospun PLGA/hydroxyapatite nanofibre scaffolds incorporated with graphene oxide. *PLoS One*. 2017;12(11): e0188352.
16. Shahnawaz Khan M, Abdelhamid HN, Wu HF. Near infrared (NIR) laser mediated surface activation of graphene oxide nanoflakes for efficient antibacterial, antifungal and wound healing treatment. *Colloids Surf B Biointerfaces*. 2015;127:281–291.
17. Senthil R, Berly R, Bhargavi Ram T, et al. Electrospun poly(vinyl) alcohol/collagen nanofibrous scaffold hybridized by graphene oxide for accelerated wound healing. *Int J Artif Organs*. 2018;41(8):467–473.
18. Zhao H, Zhang C, Wang Y, et al. Self-damaging aerobic reduction of graphene oxide by escherichia coli: role of GO-mediated extracellular superoxide formation. *Environ Sci Technol*. 2018;52(21):12783–12791.
19. Rauti R, Lozano N, León V, et al. Graphene oxide nanosheets reshape synaptic function in cultured brain networks. *ACS Nano*. 2016;10 (4):4459–4471.
20. Shim JB, Ankeny RF, Kim H, et al. A study of a three-dimensional PLGA sponge containing natural polymers co-cultured with endothelial and mesenchymal stem cells as a tissue engineering scaffold. *J Biomedical Materials*. 2014;9(4):045015.
21. Ranucci E, Capuano G, Manfredi A, et al. One-step synthesis of poly (lactic-co-glycolic acid)-g-poly-1-vinylpyrrolidin-2-one copolymers. *J Polym Sci A Polym Chem*. 2016;54(13):1919–1928.
22. Wang Y, Fu S, Li X, et al. Preparation and characterization of novel decellularized dermis matrix and hydroxyapatite composite membranes for tissue engineering applications. *J Adv Sci Letters*. 2012;17(1):108–113.
23. Summa M, Russo D, Penna I, et al. A biocompatible sodium alginate/ povidone iodine film enhances wound healing. *Eur J Pharm Biopharm*. 2018;122(p):17–24.
24. Gürgen SG, Sayın O, Çetin F, et al. Transcutaneous electrical nerve stimulation (TENS) accelerates cutaneous wound healing and inhibits pro-inflammatory cytokines. *J Inflammation*. 2014;37(3):775–784.
25. Stout DA, Yoo J, Santiago-Miranda AN, Webster TJ. Mechanisms of greater cardiomyocyte functions on conductive nanoengineered composites for cardiovascular application. *Int J Nanotechnol Nanomed*. 2012;7(undefined):5653–5669.
26. Miller DC, Thapa A, Haberstroh KM, Webster TJ. Endothelial and vascular smooth muscle cell function on poly(lactic-co-glycolic acid) with nano-structured surface features. *J Bio Mater*. 2004;25(1):53–61.
27. Abadikhah H, Naderi Kalali E, Khodi S, Xu X, Agathopoulos S. Multifunctional thin film nanofiltration membrane incorporated with reduced graphene oxide@ TiO2@ Ag nanocomposites for high desalination performance, dye retention, and antibacterial properties. *J ACS Appl Mater Interfaces*. 2019;11:23535–23545
28. Lee C-H, Chang S-H, Chen W-J, et al. Augmentation of diabetic wound healing and enhancement of collagen content using nanofibrous glucophage-loaded collagen/PLGA scaffold membranes. *J Colloid Interface Sci*. 2015;439:88–97.
29. Sali S, Mackey HR, Abdala AA, et al. Effect of graphene oxide synthesis method on properties and performance of polysulfone-graphene oxide mixed matrix membranes. *Nanomaterials (Basel)*. 2019;9(5): 769.
30. Halim A, Luo Q, Ju Y, et al. A mini review focused on the recent applications of graphene oxide in stem cell growth and differentiation. *Nanomaterials (Basel)*. 2018;8(9). 736
31. Zhou Q, Kang H, Bielec M, et al. Influence of different divalent ions cross-linking sodium alginate-polyacrylamide hydrogels on antibacterial properties and wound healing. *Carbohydr Polym*. 2018; 197:292–304.
32. Harris RD, Auletta JT, Motlagh SAM, et al. Chemical and electrochemical manipulation of mechanical properties in stimuli-responsive copper-cross-linked hydrogels. *J ACS Macro Letters*. 2013;2 (12):1095–1099.
33. Kumar PT, Jung B, Park J-K, et al. Flexible and microporous chitosan hydrogel/nano ZnO composite bandages for wound dressing: in vitro and in vivo evaluation. *ACS Appl Mater Interfaces*. 2012;4(5):2618–2629.
34. Chaloupka K, Malam Y, Seifalian AM. Nanosilver as a new generation of nanoproduct in biomedical applications. *J Trends Biotechnol*. 2010;28(11):580–588.
35. Santos CM, Mangadlao J, Ahmed F, et al. Graphene nanocomposite for biomedical applications: fabrication, antimicrobial and cytotoxic investigations. *J Nanotechnol*. 2012;23(39):395101.
36. Gharibi R, Yeganeh H, Rezapour-Lactoee A, Hassan ZM. Stimulation of wound healing by electroactive, antibacterial, and antioxidant polyurethane/siloxane dressing membranes: in vitro and in vivo evaluations. *J ACS Appl Mater Interfaces*. 2015;7(43):24296–24311. doi:10.1021/acsami.5b08376
37. Gizdavic-Nikolaidis MR, Bennett JR, Swift S, et al. Broad spectrum antimicrobial activity of functionalized polyanilines. *J Acta Biomaterialia*. 2011;7(12):4204–4209. doi:10.1016/j.actbio.2011.07.018
38. Seo GY, Hyun C, Koh D, et al. A novel synthetic material, BMM, accelerates wound repair by stimulating re-epithelialization and fibroblast activation. *Int J Mol Cell Med Sci*. 2018;19(4):pii: E1164
39. McGettrick HM, Smith E, Filer A, et al. Fibroblasts from different sites may promote or inhibit recruitment of flowing lymphocytes by endothelial cells. *Eur J Immunol*. 2009;39(1):113–125. doi:10.1002/eji.200838232
40. Li H, Chang J. Bioactive silicate materials stimulate angiogenesis in fibroblast and endothelial cell co-culture system through paracrine effect. *J Acta Biomaterialia*. 2013;9(6):6981–6991. doi:10.1016/j.actbio.2013.02.014
41. Chen S, Yang Q, Brow RK, et al. In vitro stimulation of vascular endothelial growth factor by borate-based glass fibers under dynamic flow conditions. *J Mater Sci Eng C*. 2017;73:447–455. doi:10.1016/j.msec.2016.12.099
42. SI L, Lee E-S, El-Fiqi A, Lee S-Y, Kim E-C, Kim H-W. Stimulation of odontogenesis and angiogenesis via bioactive nanocomposite calcium phosphate cements through integrin and VEGF signaling pathways. *J Biomed Nanotechnol*. 2016;12(5):1048–1062. doi:10.1166/jbn.2016.2209
43. Lin Y, Brown RF, Jung SB, Day DE. Angiogenic effects of borate glass microfibers in a rodent model. *J Biomed Mater Res A*. 2014;102 (12):4491–4499. doi:10.1002/jbm.a.35120
44. Hu J, Huang L, Zhuang X, et al. Electroactive aniline pentamer cross-linking chitosan for stimulation growth of electrically sensitive cells. *Biomacromol*. 2008;9(10):2637–2644. doi:10.1021/bm800705t
45. Jeong SI, Jun ID, Choi MJ, Nho YC, Lee YM, Shin H. Development of electroactive and elastic nanofibers that contain polyaniline and poly (L-lactide-co-ε-caprolactone) for the control of cell adhesion. *J Macromol Biosci*. 2008;8(7):627–637. doi:10.1002/mabi.v8:7
46. Cui H, Liu Y, Deng M, et al. Synthesis of biodegradable and electroactive tetraaniline grafted poly(ester amide) copolymers for bone tissue engineering. *Biomacromolecules*. 2012;13(9):2881–2889. doi:10.1021/bm300897j
47. Liu Y, Cui H, Zhuang X, et al. Nano-hydroxyapatite surfaces grafted with electroactive aniline tetramers for bone-tissue engineering. *Macromol Biosci*. 2013;13(3):356–365. doi:10.1002/mabi.201200345
48. Snyder S, DeJulius C, Willits RK. Electrical stimulation increases random migration of human dermal fibroblasts. *Ann Biomed Eng*. 2017;45(9):2049–2060. doi:10.1007/s10439-017-1849-x
49. Wang Y, Rouabhia M, Zhang Z. Pulsed electrical stimulation benefits wound healing by activating skin fibroblasts through the TGFβ1/ERK/NF-κB axis. *Biochimica et Biophysica Acta*. 2016;1860 (7):1551–1559. doi:10.1016/j.bbagen.2016.03.023

50. Kotwal A, Schmidt CE. Electrical stimulation alters protein adsorption and nerve cell interactions with electrically conducting biomaterials. *J Bio Mater*. 2001;22(10):1055–1064. doi:10.1016/S0142-9612(00)00344-6
51. Parsons JT, Horwitz AR, Schwartz MA. Cell adhesion: integrating cytoskeletal dynamics and cellular tension. *J Nature Mol Cell Biol*. 2010;11(9):633. doi:10.1038/nrm2957
52. Rackauskas G, Saygili E, Rana OR, et al. Subthreshold high-frequency electrical field stimulation induces VEGF expression in cardiomyocytes. *J Cell Transplant*. 2015;24(8):1653–1659. doi:10.3727/096368914X682783
53. Di LA, Rossetto A, Albanese M, et al. Expression of Vascular Endothelial Growth Factor (VEGF) mRNA in healthy bone tissue around implants and in peri-implantitis. *J Minerva Stomatologica*. 2013;62:1–7
54. Mak KM, Png CYM, Lee DJ. Type V collagen in health, disease, and fibrosis. *Anat Rec (Hoboken)*. 2016;299(5):613–629. doi:10.1002/ar.v299.5
55. Li J, Chen J, Kirsner R. Pathophysiology of acute wound healing. *Clin Dermatol*. 2007;25(1):9–18. doi:10.1016/j.clindermatol.2006.09.007
56. Pastar I, Stojadinovic O, Yin NC, et al. Epithelialization in wound healing: a comprehensive review. *J Adv Wound Care*. 2014;3(7):445–464. doi:10.1089/wound.2013.0473
57. Shuai C, Gao C, Feng P, et al. Boron nitride nanotubes reinforce tricalcium phosphate scaffolds and promote the osteogenic differentiation of mesenchymal stem cells. *J Biomed Nanotechnol*. 2016;12(5):934–947. doi:10.1166/jbn.2016.2224
58. Cipriani P, Di Benedetto P, Ruscitti P, et al. Impaired endothelium-mesenchymal stem cells cross-talk in systemic sclerosis: a link between vascular and fibrotic features. *Arthritis Res Ther*. 2014;16(5):442. doi:10.1186/s13075-014-0442-z
59. Sheikh AQ, Taghian T, Hemingway B, Cho H, Kogan AB, Narmoneva DA. Regulation of endothelial MAPK/ERK signalling and capillary morphogenesis by low-amplitude electric field. *J R Soc Interface*. 2013;10(78):20120548. doi:10.1098/rsif.2012.0548
60. Thakral G, LaFontaine J, Najafi B, Talal TK, Kim P, Lavery LA. Electrical stimulation to accelerate wound healing. *J Diabetic Foot Ankle*. 2013;4(1):22081. doi:10.3402/dfa.v4i0.22081
61. Cui H, Cui L, Zhang P, Huang Y, Wei Y, Chen X. In situ electroactive and antioxidant supramolecular hydrogel based on cyclodextrin/Copolymer inclusion for tissue engineering repair. *J Macromol Biosci*. 2014;14(3):440–450. doi:10.1002/mabi.201300366